Synthesis and Structures of *rac*-$Me_2Si(\eta^5$-1-indenyl$)_2Hf(NMe_2)_2$ and $\{Me_2Si(\eta^5$-1-indenyl$)(\eta^3$-2-indenyl$)\}Hf(NMe_2)_2$

Joseph N. Christopher and Richard F. Jordan*

Department of Chemistry, The University of Iowa, Iowa City, Iowa 52242

Jeffrey L. Petersen

Department of Chemistry, West Virginia University, Morgantown, West Virginia 26506

Victor G. Young, Jr.

Department of Chemistry, The University of Minnesota, Minneapolis, Minnesota 55455

Received March 24, 1997[⊗]

The amine elimination reaction of $Me_2Si(1\text{-indenyl})_2$ (**1,** $(SBI)H_2$) and $Hf(NMe_2)_4$ (**2**) affords *rac*-$Me_2Si(\eta^5$-1-indenyl$)_2Hf(NMe_2)_2$ (*rac*-**3,** *rac*-$(SBI)Hf(NMe_2)_2$) in 20% isolated yield. This reaction proceeds by initial formation of a mono(indenyl) intermediate, $(\eta^5$-$C_9H_6SiMe_2C_9H_7)$-$Hf(NMe_2)_3$ (**4**), which reacts reversibly with a second equivalent of **2** to form a binuclear complex, $\{\mu$-η^5:η^5-$Me_2Si(1\text{-indenyl})_2\}\{Hf(NMe_2)_3\}_2$ (**5**), and undergoes reversible intramolecular amine elimination to form *rac*-**3** and *meso*-**3**. The novel C_1-symmetric *ansa*-metallocene $\{Me_2Si(\eta^5$-1-indenyl$)(\eta^3$-2-indenyl$)\}Hf(NMe_2)_2$ (**6**), in which one of the indenyl groups is bridged through the 2-position, is observed as a side product in the synthesis of **3**. Complex **6** has been prepared in 21% isolated yield by thermolysis of **4** (or mixtures of **1** and **2**) at 160 °C and can be converted to $\{Me_2Si(\eta^5$-1-indenyl$)(\eta^3$-2-indenyl$)\}HfMe_2$ (**7**, 100% NMR) by reaction with $AlMe_3$. The molecular structures of *rac*-**3** and **6** have been determined by X-ray crystallography.

Introduction

We recently described the synthesis of a variety of *ansa*-metallocene bis(amide) complexes of the general type $(Cp\text{-}G\text{-}Cp)M(NR_2)_2$ (G = bridging group), including *rac*-$(EBI)Zr(NMe_2)_2$ (EBI = ethylenebis(1-indenyl)), *rac*-$(SBI)Zr(NMe_2)_2$ (SBI = $Me_2Si(1\text{-indenyl})_2$), and *rac*-$Me_2$-$Si(1\text{-}C_5H_2\text{-}2\text{-Me-}4\text{-}^t\text{Bu})_2Zr(NR_2)_2$, by amine elimination reactions of $M(NR_2)_4$ compounds and *ansa*-cyclopentadiene reagents.[1] These reactions proceed in a stepwise fashion via intermediate mono(indenyl) species (η^5-Cp-G-CpH)$M(NR_2)_3$, which undergo reversible amine elimination to yield the metallocene product. In some cases it is possible to control the *rac*/*meso* product ratio by controlling the steady-state concentration of amine in the system and, hence, the degree of reversibility. The $(Cp\text{-}G\text{-}Cp)M(NR_2)_2$ products are useful precursors to other $(Cp\text{-}G\text{-}Cp)MX_2$ compounds and can be activated for olefin polymerization.[1,2] Here we describe studies of the synthesis of *rac*-$(SBI)Hf(NMe_2)_2$ by this method and the unexpected discovery of an isomerization process leading to a novel metallocene, $\{Me_2Si(\eta^5$-1-indenyl$)(\eta^3$-2-indenyl$)\}Hf(NMe_2)_2$. Hafnium metallocenes are of interest because catalysts derived from them produce polyolefins with molecular weight higher than that obtained with analogous zirconocene catalysts.[3] *rac*-$(SBI)HfCl_2$ has been prepared in 32% yield by the reaction of $Li_2[SiMe_2(1\text{-indenyl})_2]$ with $HfCl_4$.[4]

Results and Discussion

Synthesis of *rac*-$(SBI)Hf(NMe_2)_2$ (*rac*-3). The reaction of $SiMe_2(1\text{-indenyl})_2$ ($(SBI)H_2$, **1**; 1/1 mixture of *rac* and *meso* isomers) and $Hf(NMe_2)_4$ (**2**) at 23 °C (C_6H_6 or hexanes, <30 min, system open to bubbler) yields a 4/1 mixture of mono(indenyl) species, $(\eta^5$-C_9H_6-$SiMe_2C_9H_7)Hf(NMe_2)_3$ (three isomers, **4a**−**c**), and binuclear species, $(\mu$-η^5:η^5-SBI$)\{Hf(NMe_2)_3\}_2$ (two isomers, *rac*-**5** and *meso*-**5**), as shown in Scheme 1. Removing the volatiles from this mixture and heating the resulting oil at 120 °C for 32 h under dynamic vacuum affords *rac*-$(SBI)Hf(NMe_2)_2$ (*rac*-**3**) in 58% NMR yield. The remainder of the reaction mixture contains *meso*-**3** (4.5%

[⊗] Abstract published in *Advance ACS Abstracts,* June 1, 1997.

(1) (a) Diamond, G. M.; Jordan, R. F.; Petersen, J. L. *J. Am. Chem. Soc.* **1996**, *118*, 8024. (b) Christopher, J. N.; Diamond, G. M.; Jordan, R. F.; Petersen, J. L. *Organometallics* **1996**, *15*, 4038. (c) Diamond, G. M.; Jordan, R. F.; Petersen, J. L. *Organometallics* **1996**, *15*, 4030. (d) Diamond, G. M.; Jordan, R. F.; Petersen, J. L. *Organometallics* **1996**, *15*, 4045. (e) Diamond, G. M.; Rodewald, S.; Jordan, R. F. *Organometallics* **1995**, *14*, 5.

(2) (a) Kim, I.; Jordan, R. F. *Macromolecules* **1996**, *29*, 489. (b) Jordan, R. F.; Diamond, G. M.; Christopher, J. N.; Kim, I. *Polym. Prepr. (Am. Chem. Soc., Div. Polym. Chem.)* **1996**, *37*, 256.

(3) (a) Spaleck, W.; Antberg, M.; Rohrmann, J.; Winter, A.; Bachmann, B.; Kiprof, P.; Behm, J.; Herrmann, W. A. *Angew. Chem., Int. Ed. Engl.* **1992**, *31*, 1347. (b) Spaleck, W.; Antberg, M.; Dolle, V.; Klein, R.; Rohrmann, J.; Winter, A. *New J. Chem.* **1990**, *14*, 499. (c) Kaminsky, W.; Engehausen, R.; Zoumis, K.; Spaleck, W.; Rohrmann, J. *Makromol. Chem.* **1992**, *193*, 1643. (d) Ewen, J. A.; Haspeslagh, L.; Atwood, J. L.; Zhang, H. *J. Am. Chem. Soc.* **1987**, *109*, 6544. (e) Ewen, J. A.; Haspeslagh, L.; Elder, M. J.; Atwood, J. L.; Zhang, H.; Cheng, H. N. In *Transition Metals and Organometallics as Catalysts for Olefin Polymerization* Kaminsky; W., Sinn, H., Eds.; Springer-Verlag: Berlin, 1988; p 281. (f) Gauthier, W. J.; Corrigan, J. F.; Taylor, N. J.; Collins, S. *Macromolecules* **1995**, *28*, 3771. (g) Mise, T.; Miya, S.; Yamazaki, H. *Chem. Lett.* **1989**, 1853.

(4) (a) Welborn, H. C., Jr. U.S. Patent 5,017,714, 1991. (b) Rohrmann, J.; Herrmann, W. A. Eur. Pat. Appl. 0 320 762 A2, 1988.

S0276-7333(97)00242-2 CCC: $14.00

Scheme 1

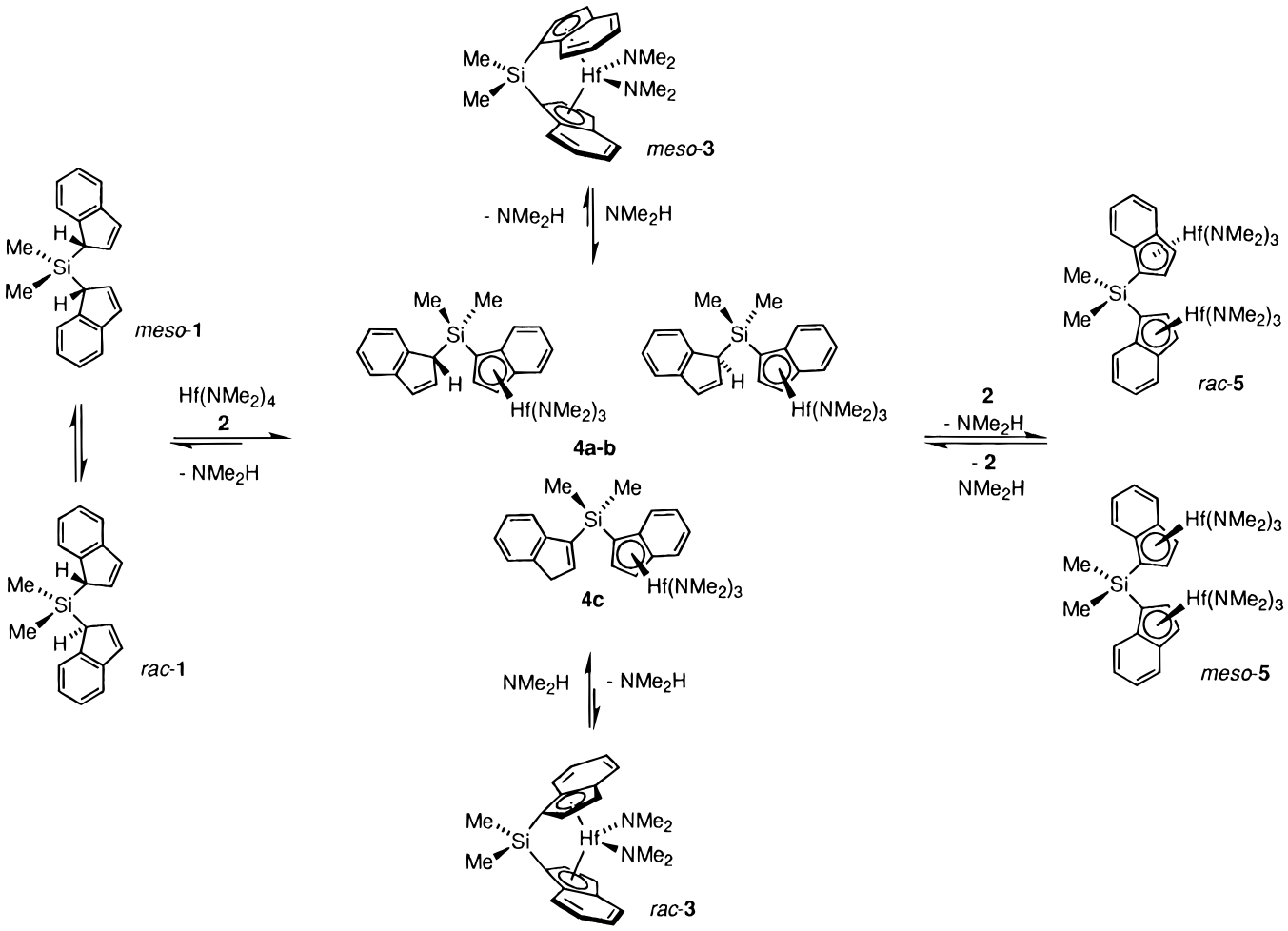

of total Hf species), **4** (7.6%), **5** (25.4%), and a new *ansa*-metallocene species in which one of the indenyl rings is attached to the bridge at the 2-position, *i.e.* {$Me_2Si(\eta^5$-1-indenyl)(η^3-2-indenyl)}$Hf(NMe_2)_2$ (**6**, 5.5%; *vide infra*). Pure *rac*-**3** was isolated by sublimation as an orange powder in 20% yield and was characterized by ^1H and ^{13}C NMR spectroscopy and an X-ray crystal structure determination. *meso*-**3** was identified by ^1H NMR spectroscopy. The ^1H NMR spectrum of C_2-symmetric *rac*-**3** contains one $SiMe_2$ and one NMe_2 resonance, while the spectrum of C_s-symmetric *meso*-**3** contains two $SiMe_2$ and two NMe_2 resonances. The synthesis of *rac*-**3** is summarized in eq 1.

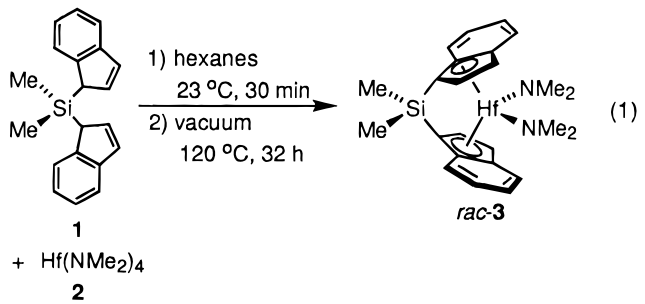

(1)

Reaction Mechanism and Practical Considerations. The mechanism and stereoselectivity of the reaction shown in eq 1 were investigated by NMR studies and model reactions. The results of these studies are consistent with the mechanism in Scheme 1, which is analogous to that established earlier for the amine elimination synthesis of *rac*-(SBI)$Zr(NMe_2)_2$.[1b] Key observations are summarized below.

(i) The reaction of **1** and **2** in C_6D_6 in a closed system (from which the evolved amine cannot escape) proceeds rapidly (1 h) at 23 °C and yields a 4/1 mixture of mono(indenyl) species **4a**−**c**, and binuclear complex **5** (1/2 *rac*/*meso* ratio), along with unreacted **1** and **2** and NMe_2H; *i.e.*, 67% of **2** ends up as **4** and 33% as **5**. After 27 h at 23 °C, the **4**/**5** product ratio decreases to 2.3/1, which is close to the statistical ratio of 2/1 expected if the indene groups react independently. The addition of NMe_2H (3 equiv based on Hf) to this mixture results in rapid (<10 min, 23 °C) conversion of **5** back to **4** and **2**. These observations indicate that the amine elimination reactions of **1** and **2** to form **4** and of **4** and **2** to yield **5** are rapid and reversible at 23 °C.

The mono(indenyl) intermediate **4** was identified by ^1H NMR spectroscopy. The three isomers of this compound differ in the site of attachment of the $SiMe_2$ bridge to the pendant indene group and the relative stereochemistry of the bridgehead carbon and the (η^5-indenyl)Hf unit. In the major isomers **4a**,**b**, the $SiMe_2$ bridge is attached at the 1-position, while in the minor isomer **4c** it is attached at the 3-position. Isomers **4a** and **4b** can be identified by the relative intensities of the two $SiMe_2$ and the allylic hydrogen resonances (3/3/1) but cannot be distinguished from each other. Isomer **4c** is distinguished from **4a**,**b** by the 3/3/2 ratio of the $SiMe_2$ and allylic hydrogen resonances.

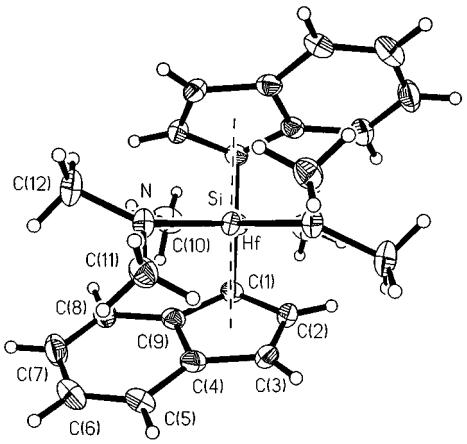

Figure 1. Molecular structure of *rac*-(SBI)Hf(NMe_2)$_2$ (*rac*-**3**).

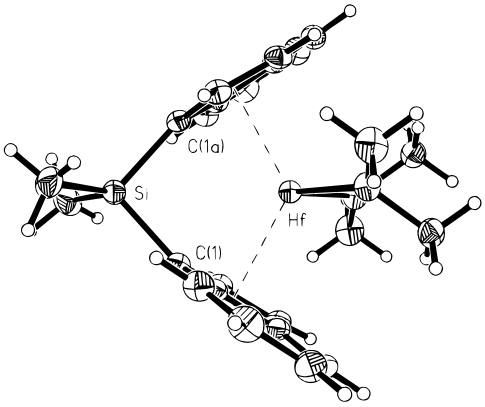

Figure 2. Alternate view of the structure of *rac*-**3**.

Complex **5** was generated in >95% NMR yield as a 1/2 *rac*/*meso* mixture by the reaction of **1** and 2 equiv of **2** (C_6D_6, 23 °C). The ^{1}H NMR spectrum of the C_s-symmetric *meso* isomer contains two $SiMe_2$ resonances, while that of the C_2-symmetric *rac* isomer contains one $SiMe_2$ resonance.

(ii) Complex **4** does not undergo intramolecular amine elimination at room temperature, even after removal of NMe_2H under vacuum. However, addition of NMe_2H (3 equiv based on Hf) to a solution of pure *rac*-**3** results in rapid (<10 min, 23 °C) conversion of *rac*-**3** to a mixture of **4** and **5**. These observations indicate that the equilibrium between **4** and **3** + NMe_2H strongly favors **4**. The conversion of **4** to **3** is probably very slow at 23 °C.

(iii) The reaction of **1** and **2** in toluene at 100 °C (21 h), *m*-xylene at 120 °C (48 h), or *m*-xylene at 140 °C (21 h), in a system equipped with an oil bubbler to allow the evolved amine to escape, yields a mixture of **4** and **5**. Similarly, the reaction of **1** and **2** in toluene (110 °C) in a flask equipped with a water-cooled fractionating column loaded with 3 mm glass helices yields only *ca.* 15% of **3** after 42 h. These observations indicate that high temperatures and efficient NMe_2H removal are required for the conversion of **4** to **3**. In our hands, thermolysis of neat **4** (containing ca. 20% **5**) provided the simplest laboratory-scale synthesis of **3**.

Structure and Bonding in *rac*-(SBI)Hf(NMe_2)$_2$ (*rac*-3). The molecular structure of *rac*-**3** was determined by X-ray diffraction (Figures 1 and 2, Tables 1 and 2). *rac*-**3** adopts a bent-metallocene structure with crystallographically imposed C_2 symmetry, which is very similar to that of *rac*-(SBI)Zr(NMe_2)$_2$ and other Me_2Si-bridged group 4 *ansa*-metallocenes.[1b,5] The centroid−Hf−centroid angle (123.3°), dihedral angle between the C_5 ring planes (63.5°), and N−Hf−N angle (96.0(2)°) of *rac*-**3** are all within 1° of the corresponding values for *rac*-(SBI)Zr(NMe_2)$_2$. Additionally, the trend in M−C bond lengths, *i.e.* M−C(2) < M−C(1) < M−C(3) < M−C(9) < M−C(4), is the same for these two *rac*-(SBI)M(NMe_2)$_2$ compounds. The lengthening of the M−C(4) and M−C(9) bonds relative to the remaining M−C bonds may be characterized as a minor slip distortion toward an η^3 bonding mode.[6] The slip parameter Δ_{av}(M−C), *i.e.* the difference between the average of the M−C(1), M−C(2), and M−C(3) bond lengths and the average of the M−C(4) and M−C(9) bond lengths, determined for *rac*-**3** (0.13 Å) is comparable to values observed for *rac*-(SBI)Zr(NMe_2)$_2$ (0.11 Å) and the unbridged analogue (η^5-indenyl)$_2$HfMe_2 (0.11 Å).[1b,7]

As illustrated in Figure 2, the Si−C(1) bond is bent 15.9° out of the plane of the five-membered indenyl ring toward the Hf center, and the C(1)−Si−C(1)′ angle (95.9(2)°) is significantly decreased from the normal tetrahedral value. These distortions from the ideal geometries expected for sp^2 C and sp^3 Si centers reflect the ring strain associated with the one-atom bridge and are typical for Me_2Si-bridged metallocenes.[5] Similar values for the Si−C/C5 plane and ring−Si−ring angles were observed for $Me_2Si(C_5H_4)_2ZrCl_2$ (16.1, 93.2(2)°) and *rac*-(SBI)Zr(NMe_2)$_2$ (15.4, 95.7(1)°).[1b,5a]

The bonding parameters for the amide groups of *rac*-**3** are consistent with partial N−Hf π-donation. The amides are flat (sum of angles around N 359.7°), and the Hf−N distance (2.057(3) Å) is in the range observed for other unsaturated Hf(IV) amide complexes (2.03−2.12 Å).[8] The dihedral angle between the N−Hf−N′ and C(11)−N−C(12) planes is 39.4°. Steric crowding between the SBI ligand framework and the NMe_2 ligands prevents the amides from adopting a more perpendicular orientation, which would maximize π-bonding.[9] Additionally, the Hf−N−C(12) angle is widened from the sp^2 value of 120° to 131.0(3)° and the C(11)−N−C(12) angle is narrowed to 109.2(3)°, presumably due to steric interactions.

Synthesis and Characterization of {Me_2Si(1-indenyl)(2-indenyl)}Hf(NMe_2)$_2$ (6). As noted above, **6** is formed as a byproduct (5−10%) in the synthesis of *rac*-**3** under the conditions illustrated in eq 1. However,

(5) (a) Bajgur, C. S.; Tikkanen, W. R.; Petersen, J. L. *Inorg. Chem.* **1985**, *24*, 2359. (b) Herrmann, W. A.; Rohrmann, J.; Herdtweck, E.; Spaleck, W.; Winter, A. *Angew. Chem., Int. Ed. Engl.* **1989**, *28*, 1511. (c) Wiesenfeldt, H.; Reinmuth, A.; Barsties, E.; Evertz, K.; Brintzinger, H. H. *J. Organomet. Chem.* **1989**, *369*, 359. (d) Burger, P.: Hortmann, K.; Diebold, J.; Brintzinger, H. H. *J. Organomet. Chem.* **1991**, *417*, 9. (e) Spaleck, W.; Antberg, M.; Rohrmann, J.; Witner, A.; Bachmann, B.; Kiprof, P.; Behm, J.; Herrmann, W. A. *Angew. Chem., Int. Ed. Engl.* **1992**, *31*, 1347. (f) Stehling, U.; Diebold, J.; Kirsten, R.; Röll, W.; Brintzinger, H. H.; Jüngling, S.; Mühlhaupt, R.; Langhauser, F. *Organometallics* **1994**, *13*, 964.

(6) Leading references: (a) Faller, J. W.; Crabtree, R. H.; Habib, A. *Organometallics* **1985**, *4*, 929. (b) Casey, C. P.; O'Connor, J. M. *Organometallics* **1985**, *4*, 384. (c) Casey, C. P.; O'Connor, J. M. *Chem. Rev.* **1987**, *87*, 307.

(7) Atwood, J. L.; Hunter, W. E.; Hrncir, D. C.; Samuel, E.; Alt, H.; Rausch, M. D. *Inorg. Chem.* **1975**, *14*, 1757.

(8) (a) Hillhouse, G. L.; Bulls, A. R.; Santarsiero, B. D.; Bercaw, J. E. *Organometallics* **1988**, *7*, 1309. (b) Zambrano, C. H.; Profilet, R. D.; Hill, J. E.; Fanwick, P. E.; Rothwell, I. P. *Polyhedron* **1993**, *12*, 689. (c) Black, D. G.; Jordan, R. F.; Rogers, R. D. *Inorg. Chem.* **1997**, *36*, 103.

(9) Lauher, J. W.; Hoffmann, R. *J. Am. Chem. Soc.* **1976**, *98*, 1729.

Table 1. Summary of Crystallographic Data for *rac*-(SBI)Hf(NMe$_2$)$_2$ (*rac*-3) and {Me$_2$Si(η^5-1-indenyl)(η^3-2-indenyl)}Hf(NMe$_2$)$_2$ (6)[a]

compd	*rac*-**3**	**6**
empirical formula	$C_{24}H_{30}HfN_2Si$	$C_{24}H_{30}HfN_2Si$
fw	553.08	553.08
temp, K	295(2)	173(2)
wavelength, Å	0.710 73	0.710 73
cryst syst	monoclinic	triclinic
space group	*C*2/*c*	$P\bar{1}$
unit cell dimens	a = 17.453(3) Å, b = 12.471(2) Å, c = 11.178(2) Å, α = 90°, β = 115.02(3)°, γ = 90°	a = 7.9483(1) Å, b = 10.2468(1) Å, c = 14.8485(1) Å, α = 78.024(1)°, β = 78.708(1)°, γ = 71.005(1)°
V, Å^3	2204.7(7)	1107.78(2)
Z	4	2
density (calcd), g/cm^3	1.666	1.658
μ, cm^{-1}	47.98	47.74
F(000)	1096	548
cryst size, mm	0.18 × 0.40 × 0.40	0.35 × 0.20 × 0.15
θ range, deg	2.08−25.00	1.42−25.00
index ranges	$-1 \le h \le 19$, $-1 \le k \le 14$, $-13 \le l \le 12$	$-9 \le h \le 9$, $-11 \le k \le 12$, $0 \le l \le 17$
no. of reflns collected	2285	6080
no. of indep rflns	1874 (R_{int} = 0.0170)	3776 (R_{int} = 0.0199)
refinement method	full-matrix least squares on F^2, all non-H anisotropic; H isotropic, fixed	full-matrix least squares on F^2, all non-H anisotropic; H isotropic, fixed
data/restraints/params	1847/0/132	3776/0/289
goodness of fit on F^2	1.085	1.032
final R indices ($I > 2\sigma(I)$)[a]	R1 = 0.0193, wR2 = 0.0462	R1 = 0.0265, wR2 = 0.0662
R indices (all data)	R1 = 0.0227, wR2 = 0.0480	R1 = 0.0294, wR2 = 0.0676
largest diff peak and hole, eÅ^3	0.619 and −0.619	1.237 and −1.429

[a] $R1 = \sum||F_o| - |F_c||/\sum|F_o|$, $wR2 = [\sum[w(F_o^2 - F_c^2)^2]/\sum[w(F_o^2)^2]]^{1/2}$.

Table 2. Selected Bond Lengths (Å) and Angles (deg) for *rac*-(SBI)Hf(NMe$_2$)$_2$ (*rac*-3)[a,b]

Hf−N	2.057(3)	Hf−C(1)	2.555(4)
Hf−C(2)	2.507(4)	Hf−C(3)	2.599(4)
Hf−C(4)	2.716(4)	Hf−C(9)	2.644(4)
Si−C(10)	1.853(5)	Si−C(1)	1.852(4)
N−C(12)	1.458(5)	N−C(11)	1.451(5)
N−Hf−N′	96.0(2)	Cp(c)−Hf−Cp′(c)	123.3
Cp(c)−Hf−N	107.6	C(1)−Si−C(1)′	95.9(2)
C(1)−Si−C(10)	113.3(2)	C(10)−Si−C(10)′	110.4(3)
C(1)−Si−C(10)′	111.7(2)	C(11)−N−Hf	119.5(3)
C(12)−N−Hf	131.0(3)	C(12)−N−C(11)	109.2(3)

[a] Symmetry transformations used to generate equivalent atoms, indicated by a prime: $-x, y, -z + 1/2$. [b] Cp(c) denotes the centroid of the five-membered ring of the indenyl group.

6 is the major product when neat **4** (containing ca. 20% **5**) or a mixture of **1** and **2** is thermolyzed at higher temperatures. Thus, the reaction of **1** and **2** in the absence of solvent at 160 °C for 24 h under dynamic vacuum affords **6** in 63% NMR yield, along with *rac*-**3** (6.0% of total Hf species), **4** (8.0%), **5** (5.0%), and an unknown species (18%).[10] Crystallization of the crude product mixture from hexanes yields pure **6** in 21% yield.

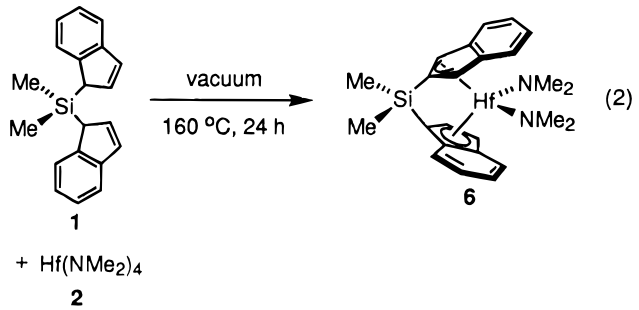

1 + Hf(NMe$_2$)$_4$ **2** → **6** (2)

The atom connectivity of **6** was established by 1-D and 2-D NMR studies. The ^{1}H and ^{13}C NMR spectra

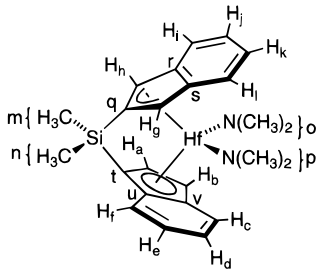

Figure 3. Labeling scheme for {Me$_2$Si(η^5-1-indenyl)(η^3-2-indenyl)}Hf(NMe$_2$)$_2$ (**6**) used in NMR assignments.

establish that **6** has C_1 symmetry; *i.e.*, the two indenyl, Si−Me, and NMe$_2$ groups are inequivalent, but the two methyl groups on a given amide ligand are equivalent. General chemical shift trends and COSY, HMQC, HMBC, and NOESY correlations allow full assignment of all ^{1}H and ^{13}C NMR resonances for **6**.[11] A labeling scheme is given in Figure 3, and NMR assignments are listed in Table 3.

The ^{1}H NMR resonances for the H$_a$−H$_f$ indenyl group are normal for an η^5-1-SiR$_2$-indenyl ligand and are very similar to the indenyl resonances of *rac*-**3**. The H$_a$ signal appears as a doublet ($^3J_{H_a-H_b}$ = 3 Hz) at δ 5.89, and the H$_b$ signal appears as a doublet of doublets at δ 6.57 (long range $^4J_{H_b-H_c}$ = 1 Hz). The $^3J_{H_a-H_b}$ value of 3 Hz is similar to values observed in other group 4 metal bis(1-indenyl) *ansa*-metallocenes.[1] The hydrogens ortho to the C$_5$ ring (H$_c$, H$_f$) appear as doublets with $^3J_{H-H}$ = 8.5 Hz. The hydrogens meta to the C$_5$ ring (H$_d$, H$_e$) appear as pseudo triplets with $^3J_{H-H}$ = 7.5 Hz. The ^{13}C NMR pattern for the H$_a$−H$_f$ indenyl ring is also nearly identical to that observed for *rac*-**3**. The resonance for

(10) The unknown species has not been isolated but is believed to be Me$_2$Si(2-indenyl)$_2$Hf(NMe$_2$)$_2$. The ^{1}H NMR spectrum contains one SiMe$_2$ resonance and one NMe$_2$ resonance in a 1/2 ratio, which is consistent with this structure.

(11) ^{1}H-detected heteronuclear multiple quantum coherence (HMQC) spectra exhibit correlations between hydrogens and directly bonded carbons. ^{1}H-detected heteronuclear multiple-bond connectivity (HMBC) spectra exhibit correlations between hydrogens and carbons which are separated by two or three bonds: (a) Bax, A.; Griffey, R. H.; Hawkins, B. L. *J. Magn. Reson.* **1983**, *55*, 301. (b) Bax, A.; Sommers, M. F. *J. Am. Chem. Soc.* **1986**, *108*, 2093. (c) Ohuchi, M.; Kohno, S. *JEOL News* **1988**, *24A*(1), 2.

Table 3. ^{1}H and ^{13}C NMR Data and Assignments for 6

^{1}H NMR (δ; J_{H-H} in Hz, intensity)	assignt	^{13}C{^{1}H} NMR (δ)	assignt
7.73 (d, ^3J = 8.6, 1 H)	H_f	133.8	C_s
7.64 (d, ^3J = 8.0, 1 H)	H_i	134.8	C_r
7.56 (d, ^3J = 8.1, 1 H)	H_l	132.0	C_u
7.45 (d, ^3J = 8.5, 1 H)	H_c	127.5	C_v
6.98 (pseudo t, ^3J = 7.4, 1.0, 1 H)	H_e	124.9	C_d
6.98 (pseudo t, ^3J = 7.3, 1.0, 1 H)	H_k	124.8	C_c
6.94 (pseudo t, ^3J = 7.4, 1.0, 1 H)	H_j	124.8	C_e
6.84 (pseudo t, ^3J = 7.5, 1.0, 1 H)	H_d	124.1	C_f
6.57 (dd, ^3J = 3.0, 1.0, 1 H)	H_b	123.2	C_k
5.90 (dd, ^4J = 2.0, 1.0, 1 H)	H_h	123.0	C_i
5.89 (d, ^3J = 3.0, 1.0, 1 H)	H_a	122.2	C_j
5.64 (dd, ^4J = 2.0, 1.0, 1 H)	H_g	121.6	C_l
2.62 (s, 6H)	H_o	120.1	C_q
2.21 (s, 6 H)	H_p	117.8	C_a
0.77 (s, 3 H)	H_n	106.3	C_b
0.51 (s, 3 H)	H_m	103.1	C_h
		97.0	C_t
		94.8	C_g
		47.3	C_o
		45.1	C_p
		−1.5	C_n
		-4.4	C_m

the bridgehead carbon C_t appears at high field (δ 97.0), the C_u and C_v resonances appear at low field (δ 132.0, 127.5) and the C_a and C_b resonances appear at an intermediate position (δ 117.8, 106.3).

In contrast, the ^{1}H NMR resonances for the H_g-H_l indenyl group are quite different from those normally observed for η^5-1-SiR_2-indenyl ligands. The resonances for the hydrogens on the five-membered ring both appear upfield, (H_g, δ 5.64; H_h, δ 5.90), similar to the resonance for H_a of the 1-indenyl ring. The H_g and H_h resonances are doublets of doublets with $^4J_{H-H} = 2$ and 1 Hz. The larger splitting is due to $J_{H_g-H_h}$ coupling and is identical in magnitude with that observed between H_3 and H_5 on the C_5 rings in *rac*-$Me_2Si(1\text{-}C_5H_2\text{-}2\text{-}Me\text{-}4\text{-}^tBu)_2Zr(NR_2)_2$ complexes ($^4J_{H_3-H_5}$ = 2 Hz; R = CH_3, C_5H_{10}, C_4H_8).[1d] The smaller splitting results from coupling of H_g with H_l and of H_h with H_i and is similar to the $^4J_{H_b-H_c}$ splitting for the 1-indenyl ring. The H_i and H_l resonances appear as doublets ($^3J_{H-H}$ = 8.0 Hz), and the H_j and H_k resonances appear as pseudotriplets ($^3J_{H-H}$ = 7.4 Hz). The H_i and H_l resonances are too broad for the small $J_{H_i-H_h}$ and $J_{H_l-H_g}$ splitting (1 Hz) to be resolved; however, H_i-H_h and H_l-H_g NOESY correlations are observed. These J_{H-H} coupling patterns and the existence of NOE correlations between H_g and H_l, and between H_h and H_i can only be achieved when the SiR_2 substituent is placed at the 2-position.

The ^{13}C NMR resonances for the H_g-H_l indenyl group are also very different from those observed for the 1-indenyl ligand or for *rac*-**3**. The resonance for the bridgehead carbon C_q appears downfield at δ 120.1, the resonances for the ring junction carbons C_r and C_s appear at low field (δ 134.8, 133.8), and the C_g (δ 94.8) and C_h (δ 103.1) resonances both appear at higher field. The C_q resonance is a triplet ($^2J_{C-H}$ = 7.4 Hz) in the gated ^{13}C {^{1}H} NMR spectrum, which indicates that this carbon experiences long-range coupling to two hydrogens (H_g and H_h) and confirms the atom connectivity proposed for **6**.

Structure and Bonding in {$Me_2Si(\eta^5$-1-indenyl)-(η^3-2-indenyl)}$Hf(NMe_2)_2$ (6). The molecular structure of **6** was determined by X-ray diffraction (Figure 4, Tables 1 and 4) to confirm the atom connectivity deduced from the NMR studies and to characterize the bonding mode of the 2-indenyl ligand. Complex **6** adopts a monomeric, bent "metallocene-like" structure which differs in several important respects from the structure of *rac*-**3**, as a result of steric crowding between the amide and indenyl ligands on the crowded side of the metallocene. Most notably, the 2-indenyl ligand in **6** is significantly slipped and is best described as being η^3-bonded, as represented in Figures 3 and 4. While the Hf−C(12), Hf−C(13), and Hf−C(16) distances (average 2.56 Å) are similar to the corresponding Hf−C distances in *rac*-**3** (average 2.55 Å), the Hf−C(15) and Hf−C(14) distances (average 2.88 Å) are beyond the limit where significant bonding interaction is expected. The slip parameter Δav(M−C) (0.32 Å) is similar to that for the η^3-fluorenyl ligand in (η^5-fluorenyl)(η^3-fluorenyl)-$ZrCl_2$ (0.28 Å).[12] The slippage of the 2-indenyl ligand to η^3 bonding results from a combination of "pivoting" at C(12), such that the angle between the Si(1)−C(12)

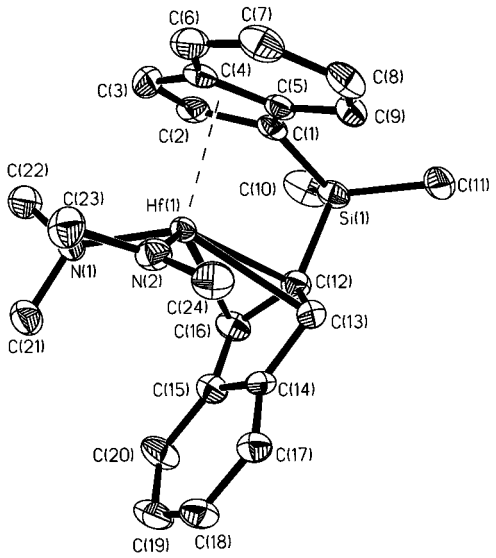

Figure 4. Molecular structure of {$Me_2Si(\eta^5$-1-indenyl)(η^3-2-indenyl)}$Hf(NMe_2)_2$ (**6**).

Table 4. Selected Bond Lengths (Å) and Angles (deg) for {$Me_2Si(\eta^5$-1-indenyl)-(η^3-2-indenyl)}$Hf(NMe_2)_2$ (6)[a]

Hf(1)−N(1)	2.049(4)	Hf(1)−N(2)	2.052(4)
Hf(1)−C(1)	2.535(4)	Hf(1)−C(2)	2.512(4)
Hf(1)−C(3)	2.541(5)	Hf(1)−C(4)	2.627(4)
Hf(1)−C(5)	2.574(4)	Hf(1)−C(12)	2.509(5)
Hf(1)−C(13)	2.538(5)	Hf(1)−C(16)	2.649(5)
Hf(1)−C(14)	2.850(4)	Hf(1)−C(15)	2.918(5)
Si(1)−C(1)	1.852(5)	Si(1)−C(10)	1.866(6)
Si(1)−C(11)	1.868(5)	Si(1)−C(12)	1.870(5)
N(1)−C(22)	1.451(6)	N(1)−C(21)	1.461(6)
N(2)−C(23)	1.461(6)	N(2)−C(24)	1.475(6)
N(1)−Hf(1)−N(2)	96.7(2)	Cp(c1)−Hf(1)−Cp(c2)	124.0
Cp(c1)−Hf(1)−N(1)	109.4	Cp(c1)−Hf(1)−N(2)	111.5
Cp(c2)−Hf(1)−N(1)	107.8	Cp(c2)−Hf(1)−N(2)	103.9
C(10)−Si(1)−C(11)	111.6(2)	C(1)−Si(1)−C(12)	95.5(2)
C(22)−N(1)−Hf(1)	134.2(3)	C(21)−N(1)−Hf(1)	117.5(3)
C(22)−N(1)−C(21)	108.3(4)	C(23)−N(2)−Hf(1)	119.5(3)
C(24)−N(2)−Hf(1)	129.6(3)	C(23)−N(2)−C(24)	109.3(4)

[a] Cp(c1) denotes the centroid of the five-membered ring of the 1-indenyl group. Cp(c2) denotes the centroid of the five-membered ring of the 2-indenyl group.

(12) (a) Kowala, C.; Wailes, P. C.; Wunderlich, J. A. *J. Chem. Soc., Chem. Commun.* **1974**, 993. (b) Kowala, C.; Wunderlich, J. A. *Acta Crystallogr.* **1976**, *B32*, 820.

bond and the C(12)−C(16) five-membered-ring plane is decreased to 6.7° (versus the normal value of *ca.* 16°), and "folding" of the five-membered ring along the C(16)−C(13) vector, such that the "fold angle" Ω between the C(16)−C(12)−C(13) and C(16)−C(15)−C(14)−C(13) planes is increased to 6.9° (versus the value of 1.6° observed for the η^5-indenyl ligands in *rac*-**3**).[13]

In contrast, the η^5-1-indenyl ligand is more symmetrically bound (Δav(M−C) = 0.07 Å) than the indenyl ligands in *rac*-**3** (Δav(M−C) = 0.13 Å). The Hf−C(4) and Hf−C(5) bonds (average 2.60 Å) are shorter than the corresponding bonds in *rac*-**3** (average 2.68 Å), which may provide some compensation for the loss of Hf−C(15) and Hf−C(14) bonding resulting from the slippage of the η^3-indenyl ligand. The Si(1)−C(1) bond is bent 17.2° out of the plane of the C(1)−C(5) ring toward the Hf center, and the C(1)−Si(1)−C(12) angle is small (95.5-(2)°).

The N(2) amide ligand, which is located on the crowded side of the metallocene, is tilted 58.8° from the perpendicular orientation which would maximize π-bonding; *i.e.*, the C(23)−N(2)−C(24)/N(1)−Hf−N(2) dihedral angle is 31.2°. The N(1) amide adopts a more perpendicular orientation (C(21)−N(1)−C(22)/N(1)−Hf−N(2) dihedral angle 47.0°). The Hf−N distances (average 2.05 Å) and the other bond lengths and angles associated with the the amide ligands are very similar to the values observed for *rac*-**3**.

Mechanism of Formation of 6. It is well established that Me_3E−indenyl compounds (E = Si, Ge, Sn) undergo [1,5]-suprafacial sigmatropic −EMe_3 shifts to generate 2-EMe_3−isoindenyl intermediates that can be trapped as Diels−Alder adducts.[14] Recently McGlinchey demonstrated that $(SBI)H_2$ undergoes *rac*/*meso* isomerization by successive [1,5]-shifts of one −$SiMe_2$(indenyl) group over the surface of the five-membered ring of the other indenyl group.[14a] The isoindene intermediate was trapped as the double-Diels−Alder adduct with tetracyanoethylene. The free energy barrier ($\Delta G^{\ddagger}$) for the [1,5]-shift was determined to be 24.2(5) kcal/mol (50 °C); *i.e.*, this process is rapid on the laboratory time scale above *ca.* 100 °C. The most likely mechanism for the formation of **6** is by a similar [1,5]-silyl shift of the mono(indenyl) species **4a**,**b** to generate isoindene species **4d** and subsequent intramolecular amine elimination (Scheme 2). The acidic hydrogen of the pendant isoindene of **4d** is expected to be more acidic and more sterically accessible than the acidic hydrogen in the indene groups of **4a**−**c** due to the loss of aromaticity in the six-membered ring and the placement of the acidic hydrogen β rather than α to the six-membered ring. Therefore, **4d** is expected to undergo more rapid amine elimination than **4a**−**c**.

Scheme 2

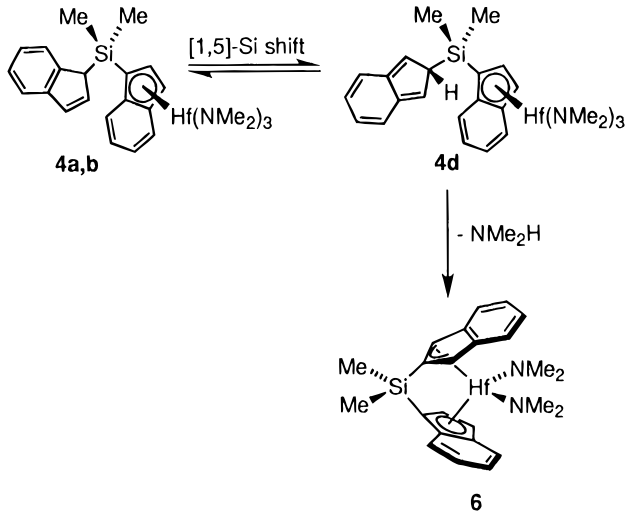

Generation of {$Me_2Si(\eta^5$-1-indenyl)(η^3-2-indenyl)}$HfMe_2$ (7). Compound **6** is cleanly converted to {Me_2-Si(η^5-1-indenyl)(η^3-2-indenyl)}$HfMe_2$ (**7**) by reaction with excess (>4 equiv) $AlMe_3$ (toluene, 23 °C, 2 h). The NMR data for **7** are very similar to the data for **6**, and therefore, these compounds are assumed to have similar structures.

Conclusions

rac-$(SBI)Hf(NMe_2)_2$ (*rac*-**3**) can be prepared with high stereoselectivity by the amine elimination reaction of $Hf(NMe_2)_4$ (**2**) and $(SBI)H_2$ (**1**). The removal of NMe_2H from the reaction mixture is the most important factor in controlling the yield of **3**. A reasonable synthesis was developed which involves the room-temperature reaction of **1** and **2** to yield a mixture of mono(indenyl) species **4** and binuclear species **5**, followed by removal of solvent and thermolysis of the neat **4**/**5** mixture under vacuum at 120 °C. Thermolysis of **4**/**5** mixtures (or of neat mixtures of **1** and **2**) at 160 °C affords the novel C_1-symmetric metallocene {$Me_2Si(\eta^5$-1-indenyl)(η^3-2-indenyl)}$Hf(NMe_2)_2$ (**6**), in which one of the indenyl groups is bridged through the 2-position. Compound **6** most likely forms by isomerization of the pendant 1-silylindene in **4** prior to the amine elimination step. Several C_2-symmetric titanocenes containing indenyl or tetrahydroindenyl ligands bridged through the 2-position by biphenyl, norbiphenyl, binaphthalene, or ethylene linkers have been described previously.[15] In these cases, the 2-substituted ligands were prepared prior to metalation. Complex **6** is topologically similar to {C_5H_4-$SiMe_2$(1-indenyl)}$HfCl_2$, {$C_5Me_4C(H)Me$(1-indenyl)}-$TiCl_2$, and related C_1-symmetric metallocenes that are precursors to catalysts which produce elastomeric polypropylene.[3f,16]

(13) In contrast, the fold angle Ω = 26° in (η^5-indenyl)(η^3-indenyl)-$W(CO)_2$: (a) Nesmeyanov, A. N.; Ustynyuk, N. A.; Makarova, L. G.; Andrianov, V. G.; Struchkov, Y. T.; Andrae, S.; Ustynyuk, Y. A.; Malyugina, S. G. *J. Organomet. Chem.* **1978**, *159*, 189. For related compounds see: (b) Ascenso, J. R.; de Azevedo, C. G.; Goncalves, I. S.; Herdtweck, E.; Moreno, D. S.; Romão, C. C.; Zühlke, J. *Organometallics* **1994**, *13*, 429. (c) Poli, R.; Mattamana, S. P.; Falvello, L. R. *Gazz. Chim. Ital.* **1992**, *122*, 315.

(14) (a) Rigby, S. S.; Girard, L.; Bain, A. D.; McGlinchey, M. J. *Organometallics* **1995**, *14*, 3798. (b) Rigby, S. S.; Gupta, H. K.; Werstiuk, N. H.; Bain, A. D.; McGlinchey, M. J. *Polyhedron* **1995**, *14*, 2787. (c) Larrabee, R. B.; Dowden, B. F. *Tetrahedron Lett.* **1970**, 915. (d) Davison, A.; Rakita, P. E. *J. Organomet. Chem.* **1970**, *23*, 407. (e) Davison, A.; Rakita, P. E. *Inorg. Chem.* **1969**, *5*, 1164. (f) Ashe, A. J., III. *Tetrahedron Lett.* **1970**, 2105. (g) Sergeyev, N. M.; Grishin, Yu. K.; Lulikov, Yu. N.; Ustynyuk, Yu. A. *J. Organomet. Chem.* **1972**, *38*, C1. (h) Lulikov, Yu. N.; Sergeyev, N. M.; Ustynyuk, Yu. A. *J. Organomet. Chem.* **1974**, *65*, 303. (i) McMaster, A. D.; Stobart, S. R. *J. Am. Chem. Soc.* **1982**, *104*, 2109. (j) McMaster, A. D.; Stobart, S. R. *J. Chem. Soc., Dalton Trans.* **1982**, 2275.

(15) (a) Halterman, R. L.; Ramsey, T. M.; Chen, Z. *J. Org. Chem.* **1994**, *59*, 2642. (b) Halterman, R. L.; Ramsey, T. M. *Organometallics* **1993**, *12*, 2879. (c) Ellis, W. W.; Hollis, K. T.; Odenkirk, W.; Whelan, J.; Ostrander, R.; Rheingold, A. L.; Bosnich, B. *Organometallics* **1993**, *12*, 4391. (d) Hitchcock, S. R.; Situ, J. J.; Covel, J. A.; Olmstead, M. M.; Nantz, M. H. *Organometallics* **1995**, *14*, 3732. (e) Nantz, M. H.; Hitchcock, S. R.; Sutton, S. C.; Smith, M. D. *Organometallics* **1993**, *12*, 5012.

Experimental Section

General Procedures. All manipulations were performed using glovebox or Schlenk techniques under a purified N_2 atmosphere. Toluene, hexane, Et_2O, and benzene-d_6 were distilled from Na/benzophenone and stored under N_2 prior to use. *m*-Xylene was distilled from molecular sieves and stored under N_2 prior to use. Me_2SiCl_2 was stirred over quinoline overnight, distilled, and stored under N_2 at 5 °C. Lithium indenide, $(SBI)H_2$, and $Hf(NMe_2)_4$ were prepared using procedures described in previous papers in this series.[1] Elemental analyses were performed by E&R Microanalytical Laboratory, Inc.

Routine NMR spectra were recorded on a Bruker AMX-360 instrument in flame-sealed or Teflon-valved tubes at 25 °C, unless otherwise indicated. ^1H and ^{13}C chemical shifts are reported versus Me_4Si and were determined by reference to the residual solvent peaks. The COSY-45, NOESY, $^1H-^{13}C$-HMQC, and $^1H-^{13}C$-HMBC NMR spectra were obtained on an Bruker AMX-600 NMR spectrometer using standard Bruker UXNMR (version 941001.2) parameter files. The spectra were processed using Felix 2.3.0 for UNIX. A mixing time of 2.0 s was used in the NOESY experiment. The gated $^{13}C\{^1H\}$ NMR spectrum of **6** was obtained on a Bruker WM-360 NMR spectrometer using Bruker Disr91 parameter files. The spectrum was processed using Felix 1.0 for Windows. For the best resolution the spectrum was processed using Line Broadening = −0.5 Hz and Gaussian Broadening = 1.0 Hz.

***rac*-(SBI)Hf(NMe$_2$)$_2$ (*rac*-3).** A solution of $Hf(NMe_2)_4$ (710 mg, 2.00 mmol) in hexanes (20 mL) was added dropwise to a solution of $(SBI)H_2$ (580 mg, 2.00 mmol) in hexanes (30 mL) at 23 °C over 5 min. The solvent was immediately (10 min) removed under vacuum, and the residual dark orange oil was heated at 120 °C under dynamic vacuum. After 24 h, *rac*-**3** had sublimed as an orange solid on the walls of the flask (220 mg, 20%). Anal. Calcd for $C_{24}H_{30}N_2SiHf$: C, 52.12; H, 5.47; N, 5.06. Found: C; 52.40; H, 5.62; N, 5.10. ^1H NMR (C_6D_6): δ 7.62 (d, J = 8 Hz, 2 H, indenyl), 7.54 (d, J = 8 Hz, 2 H, indenyl), 6.98 (pseudo t, J = 7 Hz, 2 H, indenyl), 6.82 (d, J = 3 Hz, 2 H, C_5 indenyl), 6.76 (pseudo t, J = 7 Hz, 2 H, indenyl), 6.13 (d, J = 3 Hz, 2 H, C_5 indenyl), 2.48 (s, 12 H, NMe_2), 0.79 (s, 6 H, $SiMe_2$). $^{13}C\{^1H\}$ NMR (C_6D_6): δ 131.8 (C), 130.0 (C), 125.5 (CH), 124.5 (CH), 123.9 (CH), 122.8 (CH), 115.0 (CH, C_5-indenyl), 109.1 (CH, C_5-indenyl), 96.5 (C), 47.0 (NMe_2), −1.1 ($SiMe_2$).

***meso*-(SBI)Hf(NMe$_2$)$_2$ (*meso*-3).** This species was observed by ^1H NMR as a minor product (usually *ca.* 5%) during the preparation of *rac*-**3**. ^1H NMR (C_6D_6): δ 5.99 (d, J = 3 Hz, 2 H, C_5 indenyl), 3.01 (s, 6 H, NMe_2), 1.72 (s, 6 H, NMe_2), 1.02 (s, 3 H, $SiMe_2$), 0.52 (s, 3 H, $SiMe_2$). The remaining indenyl resonances are obscured by resonances of *rac*-**3.**

(μ-η^5:η^5-SBI){Hf(NMe$_2$)$_3$}$_2$ (5). An NMR tube was charged with $(SBI)H_2$ (20 mg, 0.070 mmol), $Hf(NMe_2)_4$ (50 mg, 0.14 mmol) and C_6D_6 (0.5 mL). The tube was maintained at 23 °C for 30 h, and the contents were analyzed by ^1H NMR, which revealed the presence of *meso*-**5** (63%) and *rac*-**5** (37%). ^1H NMR (C_6D_6): *meso*-**5**, δ 7.63 (d, J = 8 Hz, 2H, indenyl), 7.59 (d, J = 8 Hz, 2H, indenyl), 6.97 (pseudo t, J = 8 Hz, 2 H, indenyl), 6.94 (pseudo t, J = 8 Hz, 2 H, indenyl), 6.45 (d, J = 3 Hz, 2 H, C_5 indenyl), 6.37 (d, J = 3 Hz, 2 H, C_5 indenyl), 2.76 (s, 36 H, NMe_2), 0.90 (s, 3 H, $SiMe_2$), 0.84 (s, 3 H, $SiMe_2$); *rac*-**5**, δ 7.50 (d, J = 8 Hz, 2 H, indenyl), 7.16 (d J = 8 Hz, 2 H, indenyl), 6.80 (pseudo t, J = 8 Hz, 2 H, indenyl), 6.78 (d, J = 3 Hz, 2 H, C_5 indenyl), 6.63 (pseudo t, J = 8 Hz, 2 H, indenyl), 6.55 (d, J = 3 Hz, 2 H, C_5 indenyl), 2.80 (s, 36 H, NMe_2), 0.91 (s, 12 H, $SiMe_2$).

(η^5-C$_9$H$_6$SiMe$_2$C$_9$H$_7$)Hf(NMe$_2$)$_3$ (4a−c). An NMR tube was charged with $(SBI)H_2$ (25 mg, 0.087 mmol), $Hf(NMe_2)_4$ (31 mg, 0.087 mmol) and C_6D_6 (0.5 mL) and maintained at 23 °C for 1 h. The ^1H NMR spectrum revealed the presence of **4a**−**c** (67%), **5** (33%), **1**, and NMe_2H. Key ^1H NMR (C_6D_6) data: **4a**, δ 6.19 (d, J = 3 Hz, 1 H, C_5 indenyl), 3.85 (s, 1 H, bridgehead), 2.77 (s, 18 H, NMe_2), 0.45 (s, 3 H, $SiMe_2$), −0.03 (s, 3 H, $SiMe_2$); **4b**, δ 3.81 (s, 1 H, bridgehead), 2.77 (s, 18 H, NMe_2), 0.56 (s, 3 H, $SiMe_2$), −0.04 (s, 3 H, $SiMe_2$); **4c**, δ 3.10 (s, 2 H, C_5), 2.80 (s, 18 H, NMe_2), 0.75 (s, 3 H, $SiMe_2$), 0.71 (s, 3 H, $SiMe_2$); the indenyl resonances are overlapped and obscured.

{Me$_2$Si(η^5-1-indenyl)(η^3-2-indenyl)}Hf(NMe$_2$)$_2$ (6). A mixture of $Hf(NMe_2)_4$ (710 mg, 2.00 mmol) and $(SBI)H_2$ (580 mg, 2.00 mmol) was heated at 160 °C under dynamic vacuum for 24 h. The crude oil was extracted with hexanes (100 mL). The extract was filtered, concentrated to 30 mL, and cooled to −40 °C. After 7 days, a pale orange solid was collected by filtration and dried under vacuum (223 mg, 21%). ^1H and ^{13}C NMR data and assignments are listed in Table 3. NMR assignments were made using 2-D NMR methods as described in detail in the Supporting Information.

{Me$_2$Si(1-indenyl)(2-indenyl)}HfMe$_2$ (7). An NMR tube was charged with **6** (14 mg, 0.025 mmol), $AlMe_3$ (10 mg, 0.14 mmol), and C_6D_6 (0.5 mL). The tube was maintained at 23 °C and monitored by ^1H NMR. After 1 h the solution was bright yellow and conversion to {Me_2Si(1-indenyl)(2-indenyl)}-$HfMe_2$ was complete. The volatiles were removed under vacuum, and the solid was washed several times with pentane to remove the aluminum compounds. ^1H NMR (C_6D_6): δ 7.46 (d, J = 8.5 Hz, 1 H, indenyl), 7.43 (d, J = 8.4 Hz, 1 H, indenyl), 7.38 (d, J = 8.4 Hz, 1 H, indenyl), 7.26 (d, J = 8.6 Hz, 1 H, indenyl), 7.06 (pseudo t, 1 H, indenyl), 7.06 (pseudo t, 1 H, indenyl), 6.97 (pseudo t, J = 7.5 Hz, 1 H, indenyl), 6.91 (pseudo t, J = 7.5 Hz, 1 H, indenyl), 6.75 (d, J = 3.0 Hz, 1 H, C_5 indenyl), 5.70 (d, J = 2.0 Hz, 1 H, C_5 indenyl), 5.67 (d, J = 3.0 Hz, 1 H, C_5 indenyl), 5.57 (d, J = 2.0 Hz, 1 H, C_5 indenyl), 0.49 (s, 3 H, SiMe), 0.36 (s, 3 H, SiMe), −0.67 (s, 3 H, HfMe), −1.62 (s, 3 H, HfMe). $^{13}C\{^1H\}$ NMR (C_6D_6): δ 138.8 (C), 134.8 (C), 132.0 (C), 127.5 (C), 124.9 (CH), 124.8 (CH), 124.8 (CH), 124.1 (CH), 123.2 (CH), 123.0 (CH), 122.2 (CH), 121.6 (CH), 120.1 (C), 117.8 (CH, C_5-indenyl), 106.3 (CH, C_5-indenyl), 103.1 (CH, C_5-indenyl), 97.0 (C), 94.8 (CH, C_5-indenyl), 47.3 (NMe_2), 45.1 (NMe_2), −1.5 (SiMe), −4.4 (SiMe).

Acknowledgment. This research was supported by the National Science Foundation (CHE-9413022; R.F.J.) and the Albemarle Corp. We wish to acknowledge John Snyder for assistance with the 2-D NMR experiments.

Supporting Information Available: Tables and text giving details of the X-ray structural analyses of *rac*-**3** and **6**, figures giving additional views of these compounds, and text and tables giving details of the 2D NMR structure determination of **6** (27 pages). Ordering information is given on any current masthead page.

OM970242G

(16) (a) Gauthier, W. J.; Collins, S. *Macromolecules* **1995**, *28*, 3779. (b) Llinas, G. H.; Day, R. O.; Rausch, M. D.; Chien, J. C. W. *Organometallics* **1993**, *12*, 1283. (c) Llinas, G. H.; Dong, S.-H.; Mallin, D. T.; Rausch, M. D.; Lin, Y.-G.; Winter, H. H.; Chien, J. C. W. *Macromolecules* **1992**, *25*, 1242. (d) Mallin, D. T.; Rausch, M. D.; Lin, Y.-G.; Dong, S.-H.; Chien, J. C. W. *J. Am. Chem. Soc.* **1990**, *112*, 2030. (e) Ewen, J. A.; Elder, M. J.; Jones, R. L.; Haspeslagh, L.; Atwood, J. L.; Bott, S. G.; Robinson, K. *Makromol. Chem., Macromol. Symp.* **1991**, *48/49*, 253. (f) Ewen, J. A. *Macromol. Symp.* **1995**, *89*, 181. (g) Gauthier, W. J.; Collins, S. *Macromol. Symp.* **1995**, *98*, 223.